

Computational Evidence for a Variable First Shell Coordination of the Cadmium(II) Ion in Aqueous Solution

Giovanni Chillemi,* Vincenzo Barone,[†] Paola D'Angelo,[‡] Giordano Mancini,[‡] Ingmar Persson,[⊥] and Nico Sanna[§]

CASPUR, Consortium for Supercomputing in Research, Via dei Tizii 6b, 00185 ROMA, Italy, and Dipartimento di Chimica, Università di Roma "La Sapienza", P.le Aldo Moro 5, 00185 ROMA, Italy, and Dipartimento di Chimica, Università di Napoli "Federico II", Complesso Universitario di Monte S. Angelo, Via Cintia, 80126 NAPOLI, Italy, and Department of Chemistry, Swedish University of Agricultural Sciences, P.O. Box 7015, SE-750 07 Uppsala, Sweden

Received: January 26, 2005; In Final Form: March 3, 2005

In this paper, we present a state-of-the-art 100 ns molecular dynamics simulation of a cadmium(II) aqueous solution that highlights a very flexible ion first coordination shell which transits between hexa- and heptahydrated complexes. From this investigation, a dynamical picture of the water exchange process emerges that takes place through an associative mechanism for the solvent substitution reaction. Our procedure starts from the generation of an effective two-body potential from quantum mechanical *ab initio* calculations in which the many-body ion–water terms are accounted for by the polarizable continuum method (PCM). This approach is computationally very efficient and has allowed us to carry out extremely long molecular dynamics simulations, indispensable to reproduce the dynamic properties of the cadmium(II) aqueous solution. Quantum mechanical *ab initio* calculations of the hexa- and heptahydrated complexes extracted from MD configurations have revealed stable minima for both clusters with the water molecules arranged in T_h and C_2 symmetries in the hexa- and heptahydrated complexes, respectively, with a slight energetic preference for the heptahydrated one. Finally, a comparison of the calculated hexa- and heptahydrated cluster IR and Raman spectra with the experimental data in the literature, has demonstrated that the IR spectroscopy is not able to distinguish between the two species, whereas the Raman spectrum of the $\text{Cd}^{2+}-(\text{H}_2\text{O})_7$ cluster provides a better agreement with the experimental data.

1. Introduction

A detailed understanding of aqueous electrolyte solutions is of fundamental importance to the chemical physics of solvation. Consequently, a substantial amount of research work has been aimed to the description of the physical properties of solutions, especially with the purpose of elucidating the coordination structure of hydrated ions.¹ Experimental techniques such as X-ray diffraction, neutron diffraction, Raman, X-ray absorption spectroscopy, and NMR have been employed to perform structural investigations of hydrated ions. However, the characterization of the dynamic properties of ions and water molecules in the bulk and in the hydration spheres is more elusive and very difficult to be obtained from experimental techniques only. On the contrary, the combined use of experimental and theoretical methods has expanded our knowledge on the water exchange mechanism of electrolyte solutions,² and it has been recently successfully applied, for example, to highlight the existence of a flexible coordination shell of water molecules around the calcium(II) ion.³ Computer simulation techniques, such as molecular dynamics (MD), are powerful tools in the analysis of both static and dynamic properties of solvated ions in solution and have been extensively used, in

the last two decades, for the study of aqueous electrolyte solutions.¹ Historically, the first studies were carried out using two-body ion–water interaction potentials with a limited number of parameters, such as Coulombic and Lennard-Jones terms. Classical MD simulations are still carried out using additive potential models, which are usually built using data obtained from experiments (i.e., solvation enthalpy or free energy) or from *ab initio* quantum mechanical calculations. However, it has been demonstrated that this class of models is not sufficiently accurate for a reliable description of the ion–solvent interaction, and the inclusion of many-body effects is crucial. Recently, *ab initio* quantum mechanics (QM) or mixed QM/molecular mechanics (MM) MD simulations have been used to circumvent the need of accurate analytical potentials⁴ even if this approach is limited both in the dimension of the systems (hundreds of atoms) and in the length of the simulation (tens of picoseconds), owing to its computational cost. Although this very limited statistic has enabled some insight into the fast exchange mechanism in the first solvation shell of the Au(I) ion in aqueous solution⁵ and of the Cu(II) ion in ammonia solution to be gained,⁶ the study of dynamic mechanisms in the nanosecond time scale is well beyond the capability of this methodology.

Recently, we demonstrated that improvements and optimizations of the polarizable continuum model (PCM) allow for a very efficient inclusion of the averaged many body ion–water effects in a two-body classical potential (effective two-body potential).⁷ In particular, we produced, for the first time, an

* To whom correspondence should be addressed. E-mail: g.chillemi@caspur.it.

[†] Università di Napoli "Federico II".

[‡] Università di Roma "La Sapienza".

[§] CASPUR.

[⊥] Swedish University of Agricultural Sciences.

effective two-body Co^{2+} –water potential to be employed in MD simulations, and validated the whole procedure investigating the hydration properties of Co^{2+} , Ni^{2+} , and Zn^{2+} by means of MD simulations. The structural and dynamical data of the ionic hydration shells have been compared with results from extended X-ray absorption fine structure (EXAFS) spectroscopy,⁸ whereas the accuracy of the effective two-body Zn^{2+} –water potential in reproducing energetic properties has been assessed by other authors.⁹ We believe that this methodology provides a very accurate description of ion–solvent interactions in the framework of a very efficient computational approach, thus allowing the study of dynamic processes occurring in the nanosecond or longer time scale.

In this context, aqueous solutions of cadmium(II) are ideal systems, since the mean residence time of water molecules in the first hydration shell is quite short (in the range 10^{-8} – 10^{-9} s) as compared to divalent first row transition ions.¹⁰ The structure of the hydrated cadmium(II) ion in aqueous solution has been the subject of several X-ray diffraction investigations, where the number of nearest neighbors was assumed to be six and which led to consistent values for the Cd–O internuclear distance.¹¹ Despite this attention, a conclusive determination of the structure of the first hydration shell of the hydrated cadmium(II) ion has not yet been achieved due also to the peculiar characteristics of this ion that is transparent to the majority of spectroscopic techniques. A strong variation of the hydration number of cadmium(II) has been observed depending on the counterion and concentration of the solution. These results indicate a large flexibility of the first hydration shell, where anions can easily replace water molecules.¹²

In this paper, we have further developed the computational procedure previously described for the generation of effective two-body ion–water potentials,⁷ and we have characterized the structural and dynamic properties of the cadmium(II) ion in aqueous solution, by means of a 100 ns long, state-of-the-art classic MD simulation. The length of the simulation allowed us to highlight an unexpected dynamic mechanism in the first cadmium(II) hydration shell, which transits between hexa- and heptahydrated complexes.

2. Computational Procedure

The three steps of the computational procedure consist of (i) generation of the cadmium(II)– H_2O ab initio potential energy surface (PES) with the inclusion of the averaged many body ion–water effects by means of the PCM; (ii) fitting of the effective two-body cadmium(II)–O and cadmium(II)–H potentials from the ab initio scans; (iii) inclusion of the effective two-body potential in the MD code and system simulation. In the following, we briefly describe the computational method, since it has been extensively discussed elsewhere.⁷

2.1. PES Calculations. All of the quantum mechanical computations have been carried out with the Gaussian 03 package,¹³ using the Hartree–Fock (HF) method with the LANL2DZ effective core potentials (ECPs) and valence basis sets¹⁴ for the cadmium ion, and the cc-pVTZ basis set¹⁵ for the water molecule. The choice of a proper basis set has been analyzed in detail in our previous work,⁷ which shows, in particular, that the cc-pVTZ basis set reproduces very accurately the charge distribution of the SPC/E water model, adopted in the MD simulations. The cadmium(II)– H_2O interaction energy shows a less deep minimum, located at a longer ion–oxygen atom distance, as compared to the Co^{2+} –, Ni^{2+} –, and Zn^{2+} – H_2O systems, thus indicating a relatively more flexible character of the cadmium(II) hydration shell. For this reason, we carried

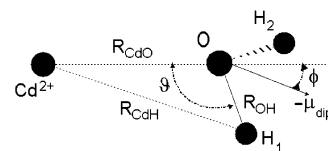


Figure 1. Cadmium(II)– H_2O geometrical parameter definition. The CdOH_1 angle ϑ is defined in the plane containing the cadmium(II), O, and H_1 atoms. μ_{dip} is the dipole water moment. The tilt angle ϕ is the angle between the cadmium(II)–O and the water dipole moment directions.

out an accurate sampling of the out of plane cadmium(II)–water interaction energy, with the inclusion of a larger number of configurations with tilt angle different from zero (see Figure 1 for the angle definitions). The PES of the cadmium(II)– H_2O system has been characterized by means of 1800 grid points with tilt angle ϕ equal to zero (ion–oxygen distances ranging from 1 to 4 Å and steps of 0.02 Å; ion–oxygen–hydrogen ϑ angles ranging from 7.745° to 127.745° and steps of 10°), and 600 grid points with tilt angle different from zero (ϕ equal to 30° , 45° , 60° , 90° , and 135° ; ion–oxygen distances ranging from 1.7 to 2.7 Å and steps of 0.1 Å; ion–oxygen–hydrogen ϑ angles ranging from 7.745° to 127.745° and step of 10°). The initial 2400 grid points were reduced to 2186 by imposing a threshold of 4000 kJ mol^{-1} for the interaction energy, thus not including the most repulsive conformations in the PES.

The PES calculation has been performed either with or without taking into account the effect of bulk solvent by means of the so-called conductor-like PCM (CPCM).¹⁶ The nonadditive effects, operative in the interaction between a water molecule and a cation, have been accounted for by the following expression for the cadmium(II)–water pair potential function (U_{CdW})¹⁷

$$U_{\text{CdW}} = \langle \psi | \hat{\mathcal{H}}^{(0)} | \psi \rangle_{\text{CdW}} - \langle \psi | \hat{\mathcal{H}}^{(0)} | \psi \rangle_{\text{Cd}} - \langle \psi | \hat{\mathcal{H}}^{(0)} | \psi \rangle_{\text{W}} \quad (1)$$

where the wave function ψ is perturbed by the solvent effect according to the CPCM, and the Hamiltonian operators \mathcal{H} refer to the cadmium(II)–water, bare cadmium(II) ion, and bare water molecule in a vacuum. The optimization of the CPCM cadmium(II) cavity radius has been performed along the line of the previously described procedure,⁷ giving rise to a cavity radius of 1.05 Å, whereas radii of 1.68 and 1.44 Å have been used for the oxygen and hydrogen atoms, respectively. Each sphere forming the solute cavity has been subdivided into finite elements (tesserae) with constant average area of 0.05 Å^2 , without any charge compensation.¹⁶

2.2. Fitting Procedure. The obtained cadmium(II)– H_2O quantum mechanical interaction energies have been fitted using the following two-body function

$$V(r) = \frac{q_i q_o}{r_{io}} + \frac{A_o}{r_{io}^4} + \frac{B_o}{r_{io}^6} + \frac{C_o}{r_{io}^8} + \frac{D_o}{r_{io}^{12}} + E_o e^{-F_o r_{io}} + \sum_{ih=ih1, ih2} \left(\frac{q_i q_h}{r_{ih}} + \frac{A_h}{r_{ih}^4} + \frac{B_h}{r_{ih}^6} + \frac{C_h}{r_{ih}^8} + \frac{D_h}{r_{ih}^{12}} \right) \quad (2)$$

where r_{io} , r_{ih1} , and r_{ih2} are the ion–water distances; q_i , q_o , and q_h are the electrostatic charges of cadmium(II), oxygen and hydrogen atoms, respectively (2, -0.8476 , and 0.4238 au); A_o , ..., F_o , A_h , ..., D_h are the unknown parameters. The SPC/E water model has been initially adopted for the MD simulation.¹⁸ As the geometry of the SPC/E model is different from the experimental one,¹⁹ adopted in the PES ab initio calculation (OH

TABLE 1: Estimate Cadmium(II)-water Interaction Parameters with Their Relative Standard Deviations

	SPC/E effective two-body		SPC/E pure pair additive		TIP5P effective two-body	
	parameters	std dev	parameters	std dev	parameters	std dev
A_o	5.577×10^{-1}	3.89×10^{-2}	5.706×10^{-1}	7.44×10^{-2}	-5.892×10^{-1}	3.47×10^{-2}
B_o	-6.130×10^{-2}	4.54×10^{-3}	-1.170×10^{-1}	9.70×10^{-3}	7.895×10^{-2}	2.86×10^{-3}
C_o	4.909×10^{-4}	6.30×10^{-5}	1.349×10^{-3}	1.16×10^{-4}	-8.682×10^{-4}	3.47×10^{-5}
D_o	-1.200×10^{-8}	3.02×10^{-9}	-5.124×10^{-8}	4.94×10^{-9}	2.938×10^{-8}	1.74×10^{-9}
E_o	$1.255 \times 10^{+6}$	$5.71 \times 10^{+4}$	$7.499 \times 10^{+5}$	$3.51 \times 10^{+4}$	$6.568 \times 10^{+4}$	$3.73 \times 10^{+3}$
F_o	$3.951 \times 10^{+1}$	4.29×10^{-1}	$3.320 \times 10^{+1}$	1.98×10^{-1}	$2.224 \times 10^{+1}$	2.17×10^{-1}
A_h	5.364×10^{-2}	1.51×10^{-3}	5.970×10^{-2}	2.10×10^{-3}	$1.797 \times 10^{+1}$	1.08×10^{-4}
B_h	2.365×10^{-4}	2.80×10^{-5}	1.682×10^{-3}	3.70×10^{-5}	-8.816×10^{-4}	1.40×10^{-5}
C_h	-1.719×10^{-6}	1.48×10^{-7}	-7.267×10^{-6}	1.82×10^{-7}	1.982×10^{-6}	4.77×10^{-8}
D_h	1.097×10^{-11}	1.09×10^{-12}	3.600×10^{-11}	1.18×10^{-12}		
A_d					1.710×10^{-1}	3.16×10^{-3}
B_d					2.340×10^{-4}	6.50×10^{-5}
C_d					1.085×10^{-5}	3.82×10^{-7}

distance of 1 Å vs 0.9572 Å; HÔH angle of 109.47° vs 104.52°, we have appropriately corrected the r_{io} and r_{ih} distances before fitting the potential of eq 2. The same fitting procedure has been carried out for a pure pair additive potential and all of the resulting cadmium(II)–SPC/E water interaction parameters are reported in Table 1, together with their standard deviations. The differences between the energies calculated with the effective two-body potential of eq 2 and the original ab initio values have a standard deviation of 16 kJ mol⁻¹, a value in agreement with other studied systems.⁷ To evaluate the influence of the water–water interactions on the MD simulations, we have performed an additional fitting using the TIP5P water model.²⁰ This model has two negative charges centered on two dummy atoms, instead of the oxygen atom, and therefore, the two-body potential function has been adapted to the following form:

$$V(r) = \frac{A_o}{r_{io}^4} + \frac{B_o}{r_{io}^6} + \frac{C_o}{r_{io}^8} + \frac{D_o}{r_{io}^{12}} + E_o e^{-F_o r_{io}} + \sum_{ih=ih1,ih2} \frac{q_i q_h}{r_{ih}} + \frac{A_h}{r_{ih}^4} + \frac{B_h}{r_{ih}^6} + \frac{C_h}{r_{ih}^8} + \sum_{id=id1,id2} \frac{q_i q_d}{r_{id}} + \frac{A_d}{r_{id}^4} + \frac{B_d}{r_{id}^6} + \frac{C_d}{r_{id}^8} \quad (3)$$

where the variables have the same meaning as in eq 2; r_{id1} and r_{id2} are the ion-dummy atom distances; q_d is the electrostatic charge of the dummy atoms (q_h and q_d are equal to +0.241 and -0.241 au, respectively). The oxygen and hydrogen atoms of the TIP5P model are in the experimental geometry, and therefore, the r_{io} and r_{ih} distances are the same of the PES calculations. The resulting cadmium(II)-TIP5P water interaction parameters, with their standard deviations are reported in Table 1.

2.3. System Setup and MD Simulation Protocol. The obtained potential functions have been included in the GRO-MACS package version 3.1 that implements efficiently parallelized MD routines with a message passing model.²¹ The computational efficiency is an important issue in the study of the cadmium(II) ion, since we are interested in the characterization of the exchanging dynamics between first and second hydration shell water molecules, which has been estimated in the nanosecond time scale.¹⁰ The study of this phenomenon, therefore, requires very large simulation time scales (≥ 100 ns), which may be faced only with efficient parallel computations. The simulated system consists of one cadmium(II) ion and 819 water molecules. A cutoff of 9 Å has been used for the nonbonded interactions, using the particle Ewald method to

correct the long-range electrostatic effects.²² The temperature was kept fixed at 300 K by weak coupling to an external temperature bath using the Berendsen's method²³ with a coupling constant of 0.1 ps. A MD simulation has been carried out with the SPC/E water model and the cadmium(II)–water effective two-body potential (eq 2 and Table 1) for 105 ns, with a time step of 1 fs (105 millions of steps). The first 5 ns have been utilized to equilibrate the system and discarded in the following analyses. This long equilibration time is mandatory for the study of dynamic phenomenon occurring in the nanosecond time scale. The trajectory of the last 100 ns has been saved every 25 ps for analyses (4 million frames). A shorter MD simulation has been carried out with the SPC/E water model and the cadmium(II)–water pure pair additive potential (eq 1 and Table 1) for 10 ns of simulation time. The trajectory of the last 5 ns has been saved every 25 ps for analyses (20 000 frames). A last MD simulation has been carried out with the TIP5P water model and the cadmium(II)–water effective two-body potential (eq 2 and Table 1) for 25 ns of simulation time. The trajectory of the last 20 ns has been saved every 25 ps for analyses (100 000 frames).

The residence times τ of water molecules in the coordination shells of the ions have been measured following the method of Impey and coauthors²⁴ and along the line of the previously described procedure.⁷ According to this method it is possible to define for each water molecule a survival probability function $P_j(t, t_n, t^*)$. This is a binary function that takes the value 1 if the water molecule j lies within the referred hydration shell at both time steps t_n and $t + t_n$ and does not leave the coordination shell for any continuous period longer than t^* . Otherwise, it takes the value 0. From P_j it is possible to define an average quantity $n_{ion}(t)$ given by the expression

$$n_{ion}(t) = \frac{1}{N_t} \sum_{n=1}^{N_t} \sum_j P_j(t_n, t, t^*) \quad (4)$$

where N_t represents the total number of steps. At long times, $n_{ion}(t)$ decays in an exponential fashion, with a characteristic correlation time τ which defines the residence time of the water molecule in the shell. We have chosen a t^* value equal to the time interval between saved configurations (25 fs). A water molecule has been considered in the first hydration shell if the cadmium(II)–oxygen distance was shorter than 3.1 Å and in the second hydration shell if the same was comprised between 3.1 and 5.4 Å.

3. Results and Discussion

The inclusion of ion–water three-body or higher-order terms is mandatory for an accurate description of the structural and

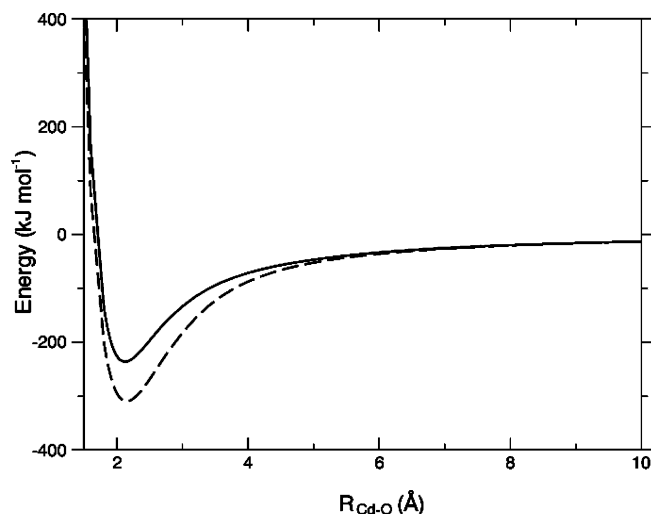


Figure 2. Fitted energy curves of the cadmium(II)–water minimum configuration as a function of the Cd–oxygen distance ($R_{\text{Cd–O}}$). The effective two-body and simple pair additive potentials are represented in full and dashed lines, respectively.

dynamical hydration properties of hydrated transition metals, and it has been recently pointed out that this is true also in the case of the cadmium(II) ion.²⁵ As previously mentioned, the inclusion of the solvent effect in the PES calculation performed according to eq 1 accounts for averaged many-body terms in an effective two-body classical potential.¹⁶ We have estimated the effect of the many-body terms in our effective two-body potential by comparing it with a pure pair additive potential, obtained by in vacuum ab initio calculations of one cadmium ion and one water molecule. The energy curves of the simple and effective two-body potentials, in the cadmium(II)–water minimum configuration, are shown in Figure 2 as a function of the ion–oxygen distance. The pure pair additive potential is more attractive, as shown by the deeper minimum, and gives rise to a longer Cd–O coordination distance as compared to the effective two-body one. Two MD simulations have been performed using the SPC/E water model and either the effective or the pure pair additive potentials of eq 2 (see Table 1). Figure 3 shows the Cd–O and Cd–H radial distribution functions $g(r)$'s obtained from the two simulations and the corresponding Cd–O structural parameters are reported in Table 2. Inspection of Figure 3 shows that the Cd–water first shell maxima are shifted toward shorter distances in going from the simple to the effective two-body potential. Moreover, in the case of the pure pair additive potential, the oxygen and hydrogen $g(r)$'s are not well separated between first and second hydration shells, indicating a disordered coordination structure around the ion. The most evident effect of the use of a pure pair additive potential concerns the oddly high number of water molecules coordinated around the cadmium(II) ion (average coordination number around eight, see Figure 3 and Table 2), in agreement with previous results.²⁵ Therefore, the inclusion of the many-body terms has a dramatic effect on the structural and dynamic properties of the cadmium(II) hydration shell. Note that our method accounts for many-body terms in a very effective way, and this allows one to carry out extremely long MD simulations which are necessary to reproduce the dynamic properties of ionic solutions with flexible hydration shells. Therefore, all of the structural and dynamic results reported in the following refer to MD simulations using the effective two-body potentials.

The average coordination number of the hydrated cadmium(II) ion obtained from the simulation with the SPC/E water model is 6.3 (see Table 2), indicating that an octahedral

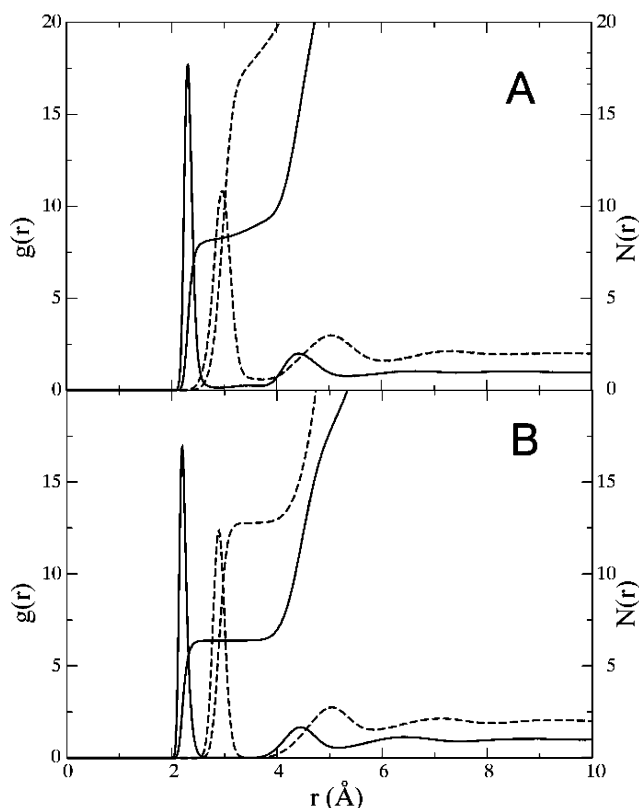


Figure 3. Radial distribution functions and corresponding hydration numbers for Cd–O (full line) and Cd–H (dashed line), obtained from the MD simulations using the simple pair additive and effective two-body potentials (panels A and B, respectively).

TABLE 2: Structural Parameters of the First and Second Cadmium(II)–O $g(r)$ Peaks^a

		first peak		second peak	
		N	$R_{\text{Cd–O}}$	N	$R_{\text{Cd–O}}$
SPC/E pure pair additive	total	8	2.33	16.8	4.57
	total	6.3	2.22	12.5	4.55
	(H ₂ O) ₆	6	2.19	12.2	4.50
	(H ₂ O) ₇	7	2.27	13.2	4.65
TIP5P effective two-body	total	6.8	2.25	13.5	4.66
	(H ₂ O) ₆	6	2.18	12.7	4.55
	(H ₂ O) ₇	7	2.26	13.7	4.69

^a N represents the coordination number; R is the mean Cd–O distance (Å). The MD results refer to the simple and effective two-body potentials with the SPC/E water model, and the effective two-body potential with the TIP5P water model. Separated $g(r)$'s for the MD frames with 6 and 7 water molecules in the first coordination shell have been considered for the simulations with the effective two-body potentials.

hydration complex is not present for the whole simulation time. Analysis on the 100 ns trajectory shows that the hydrated cadmium(II) ions transits among coordination numbers of 6, 7 and, for relatively short times, 8. In particular the $\text{Cd}^{2+}-(\text{H}_2\text{O})_6$, $\text{Cd}^{2+}-(\text{H}_2\text{O})_7$, and $\text{Cd}^{2+}-(\text{H}_2\text{O})_8$ clusters have been detected for 65.97, 34.90, and 0.13 ns, respectively, with corresponding longest lifetimes of 2297, 1048, and 10 ps. Figure 4 shows, as an example, the Cd–water coordination number as a function of time for a 5 ns simulation window (from 30 to 35 ns of simulation time). This behavior has not been observed in the only other simulation study of the hydrated cadmium(II) ion, probably due to the short simulation times (16 and 180 ps for the QM/MM and classical MD simulations, respectively).²⁵ Note that we observed the first transition between different hydration clusters after 230 ps of simulation time. Analysis on the entire 100 ns trajectory shows a relatively fast exchange process for

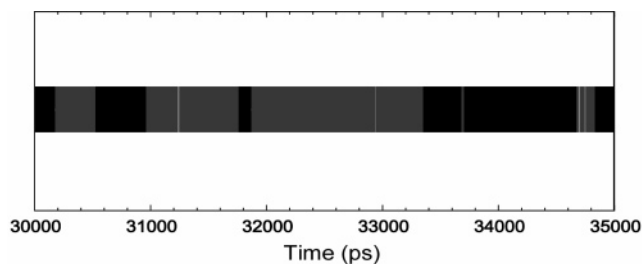


Figure 4. Cadmium(II) hydration numbers are shown as a function of simulated time. Coordination numbers of 6, 7, and 8 are represented in black, dark gray, and light gray, respectively.

the water molecules in the first hydration shell of the cadmium(II) ion, with 648 transitions between the hexa- and heptahydrated complexes and 182 transitions between hepta- and octahydrated complexes. Moreover, four transitions have been observed between simultaneously entering and leaving water molecules in the octahedral complex.

The variations of the reaction rates of the water exchange for the divalent first row transition metal ions have been described theoretically by a model assuming a pentahydrated transition state corresponding to a dissociative interchange mechanism.^{26,27} Conversely, the results for the trivalent 3d ions are consistent with an associative interchange, giving a transition state corresponding to a seven-coordinate species $M^{3+}-(H_2O)_7$.²⁶ According to the results described above, the water exchange reaction of the cadmium(II) ion follows an associative interchange mechanism with a stable heptahydrated intermediate, in line with the reported negative activation volume.¹⁰

Due to the extremely long simulation time (105 ns), we observed a very large number of water exchange events, allowing a statistically significant evaluation of the residence time of water molecules both in the first and second hydration shells of the cadmium(II) ion. Using the theoretical procedure described above, we have obtained a residence time of 3.0 ns for the first hydration shell, in agreement with the experimental values reported in the literature that indicate a first shell water residence time in the nanosecond scale.¹⁰ The residence time of the water molecules in the second hydration shell is reduced to 8 ps.

Since the $Cd^{2+}-(H_2O)_6$ and $Cd^{2+}-(H_2O)_7$ complexes are relatively stable, whereas the $Cd^{2+}-(H_2O)_8$ one is detected only for very short periods of simulation, we have separately analyzed the MD configurations in which either the hexa- or the heptahydrated species are present. The corresponding Cd–O structural parameters are reported in Table 2, whereas the Cd–O $g(r)$'s are represented in Figure 5. The Cd–O $g(r)$'s first and second shell peak maxima are located at shorter distances for the hexa-coordinated complex as compared to the heptahydrated one, and both configurations have a well ordered first shell structure, with a clear separation between the first and second peak.

The literature proposes a huge number of water models for classical MD simulations, either three-site models such as SPC,²⁸ TIP3P,²⁹ and SPC/E,¹⁸ four-site models such as TIP4P,²⁹ or five-site models such as ST2,³⁰ ST4,³¹ and TIP5P.²⁰ The existence of so many water models gives an idea of the difficulty in reproducing the peculiar structural and dynamic properties of the aqueous bulk, especially in the presence of electrolytes. Our interest does not lie in ranking the available water models but in evaluating the influence of the water–water interactions on the calculated cadmium(II)–water structural and dynamical properties. For this reason, we have repeated the Cd–water potential generation using the five-point charge TIP5P water model that reproduces remarkably well the water structural

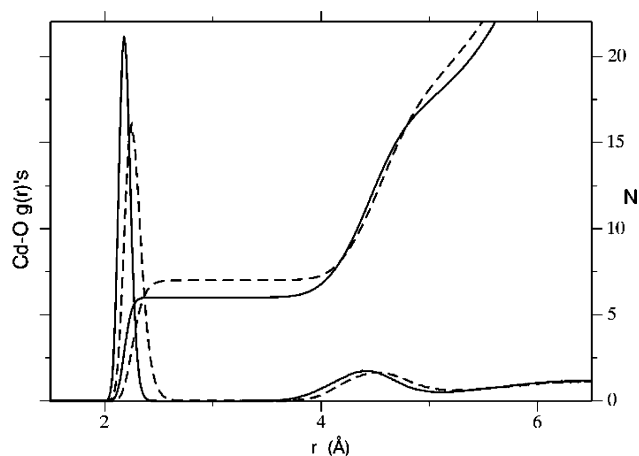


Figure 5. Cd–O radial distribution functions and corresponding hydration integration numbers for the separated MD configurations with the hexahydrated (full line) or heptahydrated (dashed line) cadmium ion.

parameters obtained from Advanced Light Source X-ray scattering experiments.³² Analysis of the 20 ns trajectory with the TIP5P model shows that the Cd–O first and second $g(r)$ peak maxima are located at slight longer distances as compared to the SPC/E results (see Table 2). A more accurate analysis of the trajectory shows the occurrence of several transitions among the $Cd^{2+}-(H_2O)_6$, $Cd^{2+}-(H_2O)_7$, and $Cd^{2+}-(H_2O)_8$ clusters in the first ionic shell, as found in the SPC/E simulation. Despite the relatively shorter time of the TIP5P simulation (25 ns), as compared to the SPC/E one (105 ns), we have also observed a statistically significant number of water exchange processes. In particular, 194 transitions between the hexa- and heptahydrated complexes and 216 between hepta- and octahydrated complexes have been detected. The $Cd^{2+}-(H_2O)_6$, $Cd^{2+}-(H_2O)_7$, and $Cd^{2+}-(H_2O)_8$ clusters are present for 3.51, 16.34, and 0.15 ns, respectively, with longest lifetimes of 220, 815, and 15 ps. The greater stability of the heptahydrated complex in the TIP5P simulation is responsible for the increase of 0.03 Å in the Cd–O $g(r)$ first peak. When considering the separate MD configurations in which either the hexa- or the heptahydrated species are present, in fact, the differences between TIP5P and SPC/E simulations are only of 0.01 Å (see Table 2). Similarly, the increase of 0.15 Å in the Cd–O $g(r)$ second peak in the TIP5P simulation is reduced to 0.05 and 0.04 Å in the separate structural parameters of the hexa- and heptahydrated complexes, respectively. Therefore, the cadmium(II)–water radial distribution functions $g(r)$'s for the hexa- and heptahydrated complexes are very similar in the simulations with either the SPC/E or the TIP5P water models. On the other hand, the water model plays an influence on the relative stabilization of the different first shell cadmium(II)–water clusters, since the six, seven, and eight coordinated water clusters are detected for 17.5, 81.7, and 0.8% of the time in the simulation with the TIP5P model, against 65.0, 34.9, and 0.1% in the SPC/E simulation. Furthermore, the water exchange events in the TIP5P simulation confirm the associative interchange mechanism for the cadmium(II) ion, but the number of water exchanges between the first hydration shell and the bulk is almost 2.5 times larger than what observed for the SPC/E model, considering a similar simulation length. This greater water mobility in the TIP5P first hydration shell leads to a value of 1.3 ns of the water residence time, which is slightly shorter than the SPC/E one (3.0 ns) but in the expected time scale. The water residence time in the second hydration shell is almost the same in the two simulations (8 and 6 ps for the SPC/E and TIP5P models, respectively).

TABLE 3: Ab Initio Energies of Hexa- and Heptahydrated Complexes

	md structures		optimized structures ^b	
	min en. PCM (a.u.)	st dev PCM (kJ/mol)	min en. in vacuo (a.u.)	min en. PCM (a.u.)
$\text{Cd}^{2+}(\text{H}_2\text{O})_6$	-502.749	13.8	-502.516	-502.833
$\text{Cd}^{2+}(\text{H}_2\text{O})_7$	-578.808	16.3	-578.594	-578.905
Δ^a	28.9 (kJ/mol)		-52.8 (kJ/mol)	-8.1 (kJ/mol)

^a $\Delta = \text{Cd}^{2+}(\text{H}_2\text{O})_7 - (\text{Cd}^{2+}(\text{H}_2\text{O})_6 + \text{H}_2\text{O})$; the ab initio optimized energies of one water molecule are -76.058 au and -76.070 au for the in vacuo and PCM calculations, respectively. ^b HF/LANL2DZ effective core potentials for the cadmium(II) ion and cc-pVTZ basis set for the water molecule.

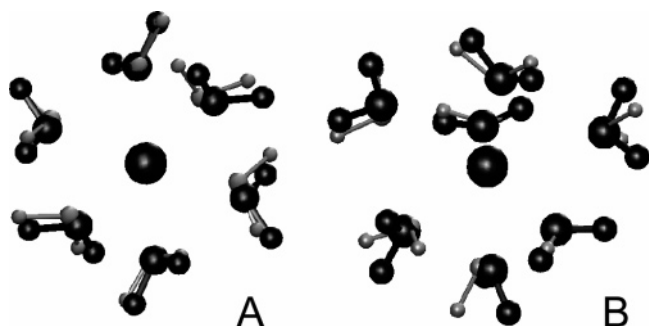


Figure 6. Perspective view of the $\text{Cd}^{2+}-(\text{H}_2\text{O})_6$ complex in T_h symmetry (panel A) and $\text{Cd}^{2+}-(\text{H}_2\text{O})_7$ complex in C_2 symmetry (panel B). The atomic positions of the ab initio PCM optimized clusters are represented in black, while the atomic positions extracted from the MD simulation are represented in gray, with smaller atom radii.

A further characterization of the $\text{Cd}^{2+}-(\text{H}_2\text{O})_6$ and $\text{Cd}^{2+}-(\text{H}_2\text{O})_7$ clusters has been carried out by extracting 1000 first shell configurations from the SPC/E simulation with the same relative ratio observed in the simulation, i.e., 650 and 350 configurations with coordination number of 6 and 7, respectively. The ab initio single-point energies of these 1000 configurations have been calculated at the same level as the PES scan (see section 2.1), and the resulting minimum energies are reported in Table 3. When the ab initio energy of a water molecule is added to the hexahydrated cluster minimum energy, we observe that the $\text{Cd}^{2+}-(\text{H}_2\text{O})_6$ cluster extracted from the MD simulation is energetically favored by 29 kJ/mol, with respect to the $\text{Cd}^{2+}-(\text{H}_2\text{O})_7$ one. We have carried out an ab initio optimization of the selected minimum configurations and found stable minima for both the $\text{Cd}^{2+}-(\text{H}_2\text{O})_6$ and $\text{Cd}^{2+}-(\text{H}_2\text{O})_7$ clusters. The $\text{Cd}^{2+}-(\text{H}_2\text{O})_6$ minimum structure shows a cadmium(II) ion surrounded by six water molecule in T_h symmetry, whereas the energy minimum configuration of the $\text{Cd}^{2+}-(\text{H}_2\text{O})_7$ complex belongs to the C_2 symmetry group, in agreement with the data reported for the $\text{V}^{3+}-(\text{H}_2\text{O})_7$ intermediate complex.²⁷ In the case of the optimized structures, we observe an inversion of the energetic preference and the heptahydrated cluster in a vacuum is favored by as much as 53 kJ mol⁻¹. This value is reduced to 8 kJ mol⁻¹ when bulk solvent effects are taken into account by means of PCM calculations on the clusters (see Table 3). The ab initio data, therefore, indicate an energetic equivalence of the two clusters, especially when considering the interaction with bulk solvent. The minimum energy structures of the hexa- and heptahydrated cadmium(II) ions are represented in Figure 6, in blue those obtained by ab initio PCM optimization calculation, and in red those extracted from the MD simulation, from which the ab initio optimization started. Figure 6 clearly shows that the atomic positions of the PCM optimized clusters are very close to the

MD starting ones (root-mean-square deviations of 1.8 and 1.9 Å, for the hexa- and heptahydrated complexes, respectively), thus indicating that the MD simulation not only identifies the existence of a variable hydration number of six and seven but it accurately samples the geometry of the hexa- and heptahydrated cadmium(II) ions around the energy minimum. Electron correlation effects on the $\text{Cd}^{2+}-(\text{H}_2\text{O})_6$ and $\text{Cd}^{2+}-(\text{H}_2\text{O})_7$ clusters have been evaluated by comparing the ab initio energies and structures obtained at the Hartree–Fock level, with analogous calculation at MP2 level.³³ The MP2 data confirm that both clusters are energy minima and that the $\text{Cd}^{2+}-(\text{H}_2\text{O})_7$ complex is the most stable one. In fact, the in vacuum energy difference between the hexa- and heptahydrated clusters is 43 kJ mol⁻¹ (to be compared to 53 kJ mol⁻¹ from HF calculations). The interaction energies of the same 1000 first shell configurations, extracted from the SPC/E simulation and utilized for the QM evaluation, have been also calculated with the effective two-body cadmium(II)–water potential. The average energy standard deviations obtained with the effective two-body potential are 12 and 13.2 kJ mol⁻¹ for the hexa- and the heptahydrated clusters, respectively, whereas the corresponding values obtained with the ab initio calculations are 13.8 and 16.3 kJ mol⁻¹ (see Table 3). The closeness of these values demonstrates that the classic effective two-body potential well reproduces the energy distribution of the ab initio QM energies. Moreover, the value of the QM standard deviations shows that the energy distributions of the first shell clusters visited by the MD simulation is significantly wider than the energy gap between the $\text{Cd}^{2+}-(\text{H}_2\text{O})_6$ and $\text{Cd}^{2+}-(\text{H}_2\text{O})_7$ clusters, thus explaining the ability of the MD simulations to sample the different cluster configurations.

The nature of the $\text{Cd}^{2+}-(\text{H}_2\text{O})_6$ and $\text{Cd}^{2+}-(\text{H}_2\text{O})_7$ energy minima, obtained at the HF level, has been further investigated by means of harmonic frequency calculations. We have then plotted, in Figure 7, the theoretical infrared (IR) and Raman spectra of the hydrated cadmium(II) ion in aqueous solution for the $\text{Cd}^{2+}-(\text{H}_2\text{O})_6$ and $\text{Cd}^{2+}-(\text{H}_2\text{O})_7$ clusters. The experimental IR spectrum, discussed in terms of the $\text{Cd}^{2+}-(\text{H}_2\text{O})_6$ complex (T_h symmetry), shows a strong band at 364 cm⁻¹ and two weak bands at 155 and 95 cm⁻¹, all of T_u type.³⁴ Our theoretical spectrum of the hexahydrated cluster shows two very strong bands of T_u symmetry at 417 and 531 cm⁻¹ and an extremely weak band at 271 cm⁻¹ (Figure 7, panel A, black bars), in agreement with Rudolph's calculations.³⁵ The theoretical IR spectrum of the heptahydrated cluster (Figure 7, panel A, white bars) presents, in the same frequency region, a larger number of bands of comparable intensity. One has further to consider that the experimental vibrational spectra of ionic systems in aqueous solution show absorptions having large half-width bands, ranging from 50 to 100 cm⁻¹.

For this reason we have simulated the IR spectra assuming a half-width of 100 cm⁻¹, obtaining the curves reported in Figure 7 (panel A) in full and dotted lines for the $\text{Cd}^{2+}-(\text{H}_2\text{O})_6$ and the $\text{Cd}^{2+}-(\text{H}_2\text{O})_7$ clusters, respectively. Both curves are consistent with the experimental data, and therefore, it seems quite difficult to distinguish between the two species by means of IR spectroscopy. Considering the Raman spectrum of the hydrated cadmium(II) ion in aqueous solution, the experimental data show a strong band at 358 cm⁻¹, with full width at half-height of 58 cm⁻¹.³⁵ The calculated Raman spectrum of $\text{Cd}^{2+}-(\text{H}_2\text{O})_6$ (Figure 7, panel B, black bars) consists of four bands in the 150–450 cm⁻¹ range. In particular, the most intense ones are those at 397 and 240 cm⁻¹, both of T_g symmetry, and at 299 cm⁻¹ of A_g symmetry, in agreement with those calculated by

- (3) Jalilehvand, F.; Spångberg, D.; Lindqvist-Reis, P.; Hermansson, K.; Persson, I.; Sandström, M. *J. Am. Chem. Soc.* **2001**, *123*, 431–441.
- (4) Erras-Hanauer, H.; Clark, T.; van Eldik, R. *Coord. Chem. Rev.* **2003**, *238–239*, 233–253.
- (5) Armunanto, R.; Schwenk, C. F.; Tran, H. T.; Rode, B. M. *J. Am. Chem. Soc.* **2004**, *126*, 2582–2587.
- (6) Christian F. Schwenk, Rode B. M. *Chem. Phys. Phys. Chem.* **2004**, *5*, 342–348.
- (7) Chillemi, G.; D'Angelo, P.; Pavel, N. V.; Sanna, N.; Barone, V. *J. Am. Chem. Soc.* **2002**, *124*, 1968–1976.
- (8) D'Angelo, P.; Barone, V.; Chillemi, G.; Sanna, N.; Meyer-Klaucke, W.; Pavel, N. V. *J. Am. Chem. Soc.* **2002**, *124*, 1958–1967.
- (9) Arab, M.; Bougeard, D.; Smirnov, K. S. *Chem. Phys. Lett.* **2003**, *379*, 268–276.
- (10) Richens, D. T. *The Chemistry of Aqua Ions*; John Wiley & Sons: New York, 1996.
- (11) (a) Bol, W.; Gerrits, G. J. A.; van Panthaleon van Eck, C. L. *J. Appl. Crystallogr.* **1970**, *3*, 486–492. (b) Ohtaki, H.; Maeda, M.; Ito, S. *Bull. Chem. Soc. Jpn.* **1974**, *47*, 2217–2221. (c) Caminiti, R.; Johansson, G. *Acta Chem. Scand.* **1981**, *A35*, 373–381.
- (12) (a) Marcus, Y. *Pure Appl. Chem.* **1987**, *59*, 1093–1101. (b) Howell, I.; Neilson, G. W. *J. Phys.: Condens. Matter* **1996**, *8*, 4455–4463.
- (13) Frisch, M. J.; Trucks, G. W.; Schlegel, H. B.; Scuseria, G. E.; Robb, M. A.; Cheeseman, J. R.; Montgomery, J. A., Jr.; Vreven, T.; Kudin, K. N.; Burant, J. C.; Millam, J. M.; Iyengar, S. S.; Tomasi, J.; Barone, V.; Mennucci, B.; Cossi, M.; Scalmani, G.; Rega, N.; Petersson, G. A.; Nakatsuji, H.; Hada, M.; Ehara, M.; Toyota, K.; Fukuda, R.; Hasegawa, J.; Ishida, M.; Nakajima, T.; Honda, Y.; Kitao, O.; Nakai, H.; Klene, M.; Li, X.; Knox, J. E.; Hratchian, H. P.; Cross, J. B.; Adamo, C.; Jaramillo, J.; Gomperts, R.; Stratmann, R. E.; Yazyev, O.; Austin, A. J.; Cammi, R.; Pomelli, C.; Ochterski, J. W.; Ayala, P. Y.; Morokuma, K.; Voth, G. A.; Salvador, P.; Dannenberg, J. J.; Zakrzewski, V. G.; Dapprich, S.; Daniels, A. D.; Strain, M. C.; Farkas, O.; Malick, D. K.; Rabuck, A. D.; Raghavachari, K.; Foresman, J. B.; Ortiz, J. V.; Cui, Q.; Baboul, A. G.; Clifford, S.; Cioslowski, J.; Stefanov, B. B.; Liu, G.; Liashenko, A.; Piskorz, P.; Komaromi, I.; Martin, R. L.; Fox, D. J.; Keith, T.; Al-Laham, M. A.; Peng, C. Y.; Nanayakkara, A.; Challacombe, M.; Gill, P. M. W.; Johnson, B.; Chen, W.; Wong, M. W.; Gonzalez, C.; Pople, J. A. *Gaussian 03*, revision B.01; Gaussian, Inc.: Pittsburgh, PA, 2003.
- (14) (a) Hay, P. J.; Wadt, W. R. *J. Chem. Phys.* **1985**, *82*, 270–283. (b) Wadt, W. R.; Hay, P. J. *J. Chem. Phys.* **1985**, *82*, 284–298. (c) Hay, P. J.; Wadt, W. R. *J. Chem. Phys.* **1985**, *82*, 299–310.
- (15) Wilson, A.; van Mourik, T.; Dunning Jr., T. H. *J. Mol. Struct. (THEOCHEM)* **1996**, *388*, 339–349.
- (16) Cossi, M.; Rega, N.; Scalmani, G.; Barone, V. *J. Comput. Chem.* **2003**, *24*, 669–681.
- (17) Floris, F.; Persico, M.; Tani, A.; Tomasi, J. *Chem. Phys. Lett.* **1992**, *199*, 518–524.
- (18) Berendsen, H. J. C.; Grigera, J. R.; Straatsma, T. P. *J. Phys. Chem.* **1987**, *91*, 6269–6271.
- (19) Benedict, W. S.; Gailar, N.; Plyler, E. K. *J. Chem. Phys.* **1956**, *24*, 1139–1165.
- (20) Mahoney W.; Jorgensen, W. L. *J. Chem. Phys.* **2000**, *112*, 8910–8922.
- (21) Berendsen, H. J. C.; van der Spool, D.; van Drunen, R. *Comput. Phys. Comm.* **1995**, *95*, 43–56.
- (22) (a) Darden, T.; York, D.; Pedersen, L. *J. Chem. Phys.* **1993**, *98*, 10089–10092. (b) Essmann, U.; Perera, L.; Berkowitz, M. L.; Darden, T.; Lee, H.; Pedersen, L. G. *J. Chem. Phys.* **1995**, *103*, 8577–8592.
- (23) Berendsen, H. J. C.; Postma, J. P. M.; van Gusteren, W. F.; Di Nola, A.; Haak, J. R. *J. Comput. Phys.* **1984**, *81*, 3684–3690.
- (24) Impey, R. W.; Madden, P. A.; McDonald, I. R. *J. Phys. Chem.* **1983**, *87*, 5071–5083.
- (25) Kritayakornupong, C.; Plankensteiner, K.; Rode, B. M. *J. Phys. Chem. A* **2003**, *107*, 10330–10334.
- (26) Åkesson, R.; Pettersson, L. G. M.; Sandström, M.; Wahlgren, U. *J. Am. Chem. Soc.* **1994**, *116*, 8705–8713.
- (27) Rotzinger, F. P. *J. Am. Chem. Soc.* **1997**, *119*, 5230–5238.
- (28) Berendsen, H. J. C.; Postma, J. P. M.; van Gunsteren, W. F.; Hermans, J. *Intermolecular Forces*; D. Reidel Publishing Company: Dordrecht, The Netherlands, 1981; pp 331–342.
- (29) Jorgensen, W. L.; Chandrasekhar, J.; Madura, J. D.; Impey, R. W.; Klein, M. L. *J. Chem. Phys.* **1983**, *79*, 926–935.
- (30) Stillinger, F. H.; Rahman, A. *J. Chem. Phys.* **1974**, *60*, 1545–1557.
- (31) Head-Gordon, T.; Stillinger, F. H. *J. Chem. Phys.* **1993**, *98*, 3313–3327.
- (32) Sorenson, J. M.; Hura, G.; Glaeser, R. M.; Head-Gordon, T. *J. Chem. Phys.* **2000**, *113*, 9149–9161.
- (33) See, for example: Saebo, S.; Almlof, J. *Chem. Phys. Lett.* **1989**, *154*, 83–89.
- (34) Mink, J.; Németh, C.; Hajba, L.; Sandström; Goggin, P. L. *J. Mol. Struct.* **2003**, *661–662*, 141–151.
- (35) Rudolph, W. W.; Pye, C. C. *J. Chem. Phys.* **1998**, *102*, 3564–3573.
- (36) D'Angelo, P.; Chillemi, G.; Barone, V.; Mancini, G.; Sanna, N.; Persson, I. *J. Phys. Chem. B*, **2005**, *109*, 9178–9185.